Article:
Mohammed, A., Marshall, M.B. and Lewis, R. (2015) Development of a method for assessing erosive wear damage on dies used in aluminium casting. Wear, 332. pp. 1215-1224. ISSN 0043-1648

https://doi.org/10.1016/j.wear.2014.12.038

Development of a Method for Assessing Erosive Wear Damage on Dies used in Aluminium Casting

A. Mohammed, M.B. Marshall, R. Lewis*

The Department of Mechanical Engineering, The University of Sheffield, Mappin Street, S1 3JD, UK.

*roger.lewis@sheffield.ac.uk

ABSTRACT

During pressure die casting of aluminium, molten/semi-solid droplets of aluminium come into contact with the die surface. A number of damage mechanisms can occur as a result of this event, some related to thermal effects and some mechanical effects such as erosion. Dies are very expensive to manufacture and options for improving die life would be beneficial.

Very few test methods exist to study the damage mechanisms and for trialling new materials/coatings. Most studies have involved either casting actual components or placing material specimens in a die casting machine so that they are impacted by the aluminium. This is very time consuming and expensive.

In this work a laboratory test was developed specifically to study the erosion effects of the aluminium particles. A mounting frame was utilised to hold both flat and cylindrical specimens made from H13 steel (typically used for die manufacture). The frame was placed in a shot blaster which was used to fire aluminium balls (3mm diameter – based on aluminium droplet size calculations) at the specimens. Different velocities were used and the flow was pulsed to mimic successive castings being made.

Flat specimens were tested at different angles and cylindrical specimens were tested central to the flow of aluminium and in an eccentric position to cover a range of possible aluminium/die impact scenarios. Optical microscopy and roughness measurements were used to characterise the wear on the specimens. Wear rates were also determined. Behaviour was compared with data from the literature where available. Wear damage was also compared with worn dies. High speed videoing was also used to study the impact behaviour of the aluminium balls.

It was concluded that the test method was a suitable approach to use in identifying potential solutions that could extend die life. In future work the effects of temperature and application of coatings will be explored.

Keywords: aluminium casting, die erosion, test development

1 INTRODUCTION

Die casting is a high volume production process in which molten metal is forced into a die under pressure. There are many advantages to using this manufacturing approach [1]. Excellent dimensional accuracy and surface finishes can be can be achieved without any machining except

to remove flash around the edges and drill/tap holes. Very complex shapes can be made and hollow sections and internal cavities can be included. Fine grain structures and good mechanical properties can also be realised.

The process is fast and economical compared to other techniques for manufacturing metal components such as forging or rolling [2]. Die casting is particularly appropriate when a large quantity of small to medium sized parts is needed with good detail and dimensional consistency and a fine surface quality [3]. The down sides are that there are long lead times due to die manufacture, large parts and high melting point materials cannot be accommodated and if parameters are not optimised there can be problems with porosity.

Most castings are made from non-ferrous materials, but ferrous materials can also be cast. In this work the focus is on high pressure casting of aluminium.

1.1 Aluminium Die Casting Process

There are a number of methods available for casting including hot and cold chamber, with and without the use of high pressure. Here high pressure, cold chamber casting of aluminium is considered. A typical layout for a cold chamber machine is shown in Figure 1 [1].

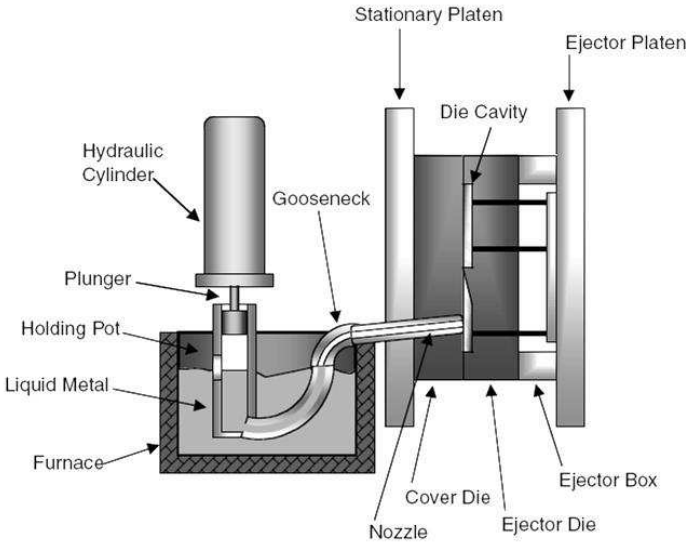

Figure 1. Schematic of a Cold-Chamber Casting Machine [1]

The molten metal is taken from an external furnace and is poured into a shot sleeve. A plunger then pushes the metal through a runner and gate into the die cavity under high pressure. This usually happens in three phases. In the first the plunger moves at low speed to push air out of the sleeve, the speed then rises to get the metal to fill the runner system and finally high speed is used as the metal is entering the die cavity. It is very important these phases are well controlled as entrapped air can lead to porosity in the castings. The high pressure used ensures that proper fill occurs and minimises shrinkage. The casting is left to solidify before the die is opened and the part removed and the process starts again.

Casting techniques are developing continuously, largely in order to achieve greater control over the main variables such as the metal used, inlet temperatures, pressures used and shot speed in order to improve throughput and avoid problems such as porosity [4].

1.2 Dies

For every component to be manufactured a new die must be made. This is an expensive process (typically tens of thousands of pounds) and represents a large investment for a casting company. As a result the dies must last for a long time and maintain high component quality. The die design is complex as it must be made in two parts to allow separation after the process is complete to allow removal of the casting. Good flow of the metal must be ensured and dimensional allowance for shrinkage etc. must be built in. The die also has to be able to endure harsh operating conditions. The molten metal is injected under pressure at high temperature (the melting point of aluminium for example is 700°C) which occurs in cycles. Dies are usually made from H13 steel which has the right mix of good machinability, strength and resistance to thermal fatigue and erosion, its properties are listed in Table 1.

Property	Value
Tensile Strength (MPa)	1650
Elongation at Break	9%
Poisson's Ratio	0.3
Hardness (H_V)	300-400
Modulus of Elasticity (GPa)	210

Table 1. Properties of H13 Steel

Die life is affected by a number of degradation mechanisms: thermal fatigue (as a result of the temperature cycles); erosion; erosion-corrosion; chemical attack and soldering [5]. All result from the contact of the molten metal with the die surface. In this study the main focus was on erosion due to the impact of molten or semi-solid metal droplets on the die as the metal is forced into the die under high pressure. The results of both thermal fatigue (cracking) and erosion (pits/gouges) are visible on the images shown in Figure 2 of used dies. While erosion may be the most significant cause of failure, mechanisms coexist and interact and often evidence will be found of several on a die surface [6]. As can be seen the metal droplets are impacting a variety of surface geometries which will have a large effect on the surface damage that results.

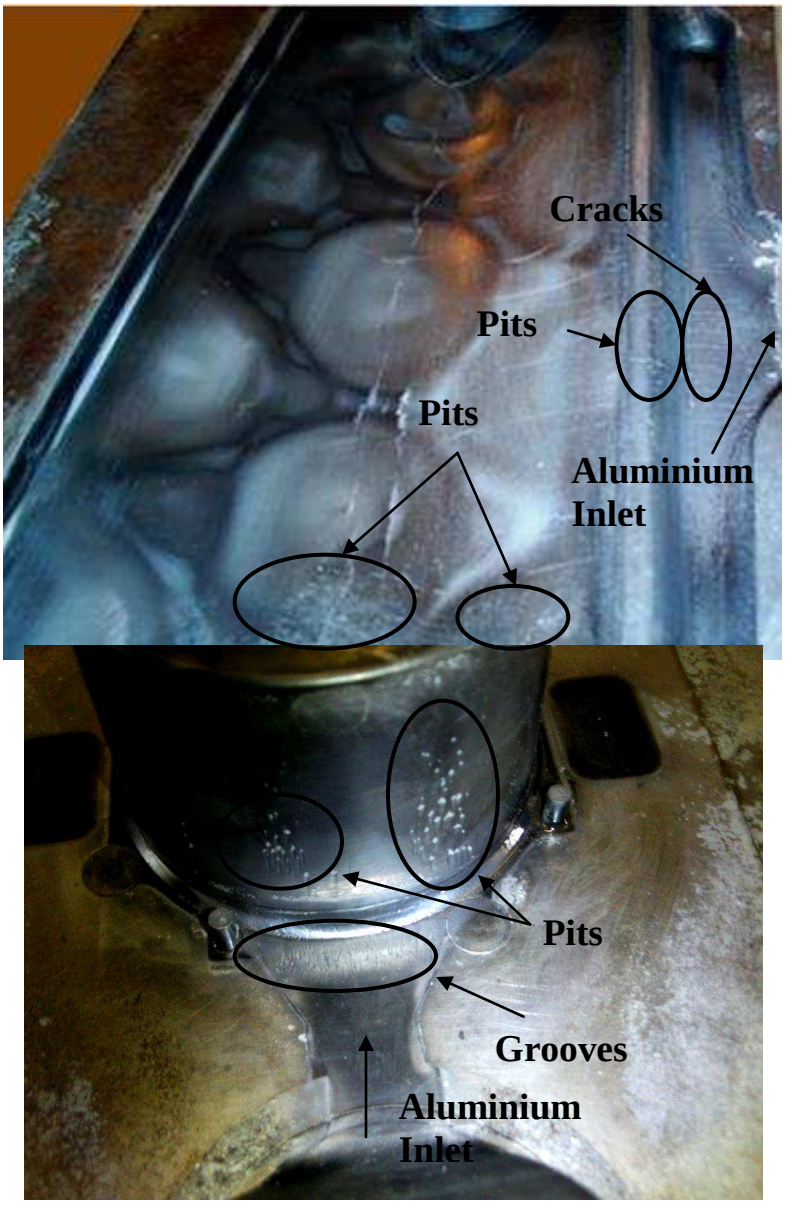

Figure 2. Damage due to Erosion and Thermal Fatigue

1.3 Previous Die Test Methods

Despite the investment made in dies, less attention has been paid to the development of solutions to reduce the impact of the failure mechanisms than has been placed on process control. The work that has been carried out has used a range of techniques across different levels of complexity, largely to assess the application of coatings to the dies or surface hardening. In order to assess the effect of coating the dies many tests have been carried out using scratch testing techniques [7-10]. These tests are easy and quick to carry out and can provide a good way of ranking coating/treatment performance, however, they do not represent the actual test conditions or failure mechanisms, so are actually quite limited.

An erosive test has been run based on ASTM standard G76-95 [11]. However, the erodent used was silica which is quite angular in nature and would give different behaviour to aluminium droplets. A different "erosive" approach has been used which involves rotating specimens at high speed (800rpm) in molten aluminium [10]. However, as before, this is not representative of the situation in the actual die where molten/semi-solid droplets are impacting the surfaces.

In order to expose potential solutions to actual operating conditions, a test was developed that allowed a holder with multiple treated/coated pins to be placed in an actual casting machine [12]. Testing has also been carried out using actual dies which are sectioned and examined after use in a casting machine. While these methods enable testing in an actual casting environment, they are costly and very time consuming. Apart from the specimen manufacture, it will not always be economically viable to have a casting machine set aside purely for research purposes. Because of the nature of these tests, it was impossible to keep stopping them to evaluate the deterioration of the dies with time, so this would also be an important consideration in the development of a new test.

Clearly there is scope for the development of a test that is more representative than the laboratory based tests reviewed above, whilst being are easier to carry out than the tests developed involving actual casting machines.

1.4 Aim and Objectives of this Work

The main aim of this work was to develop a new test approach for assessing erosive damage caused to die surfaces that can be implemented within a laboratory environment.

The objectives were to set-up the test approach; decide what the best erodent is and how to apply it in a representative way; determine the best counterface to use to mimic the varying geometry found in a die; carry out high speed video trials to assess erodent interactions with the counterface and then carry out wear tests to assess wear behaviour with time while varying parameters such as erodent contact angle and velocity, and develop test methodologies that can be used in the future to assess the effect on wear of potential die coatings and treatments.

2 TEST APPARATUS

2.1 Rig Structure

The rig was based around a commercial shot-blaster (see Figure 3). This provided the means to blast the erodent at the test surface as well as recirculate it. A frame was constructed (300mm by 300mm) that allowed the counterface to be mounted near the shot-blaster nozzle and be rotated to set different erodent impact angles.

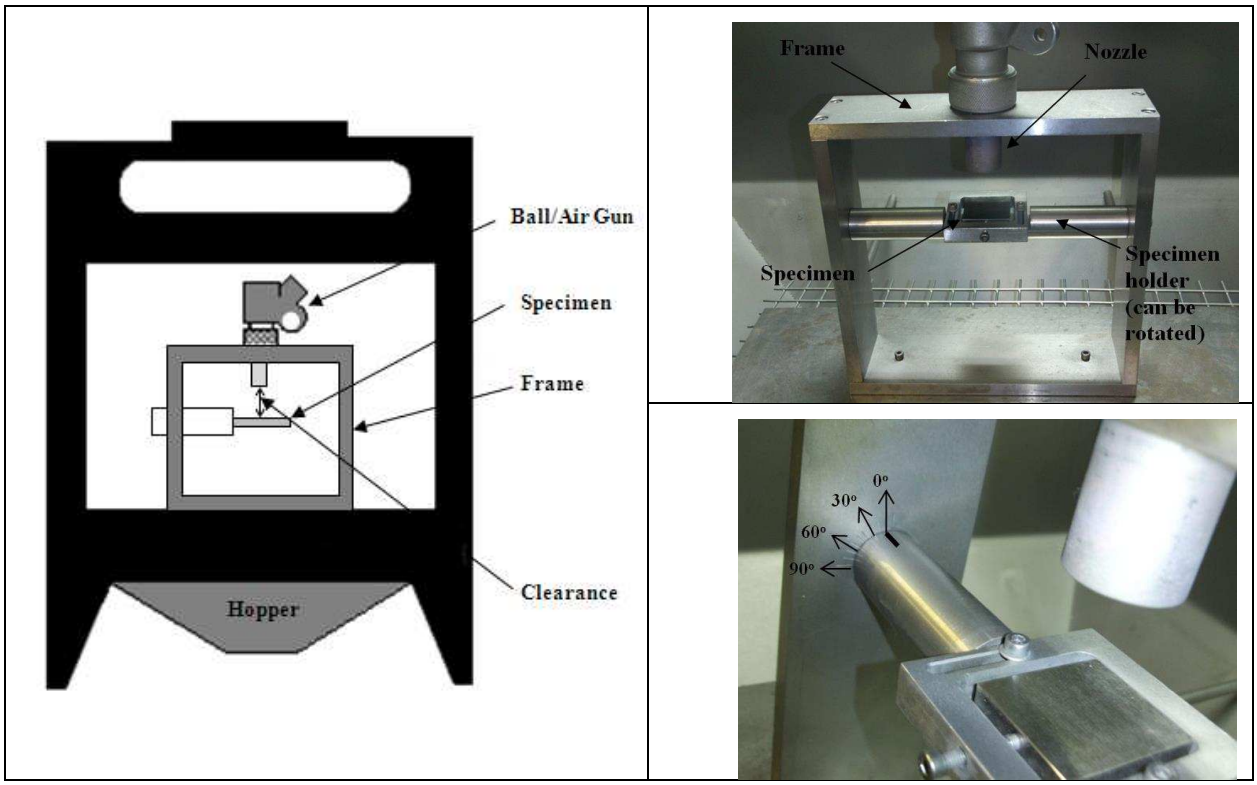

Figure 3. Test Arrangement: (a) Schematic of Overall Test Set-up (with cylindrical specimen mounted); (b) Test Surface Mounting Frame

The centre of the nozzle was placed 30mm away from the test surface in this work. It is known that the distance has an effect on the wear that occurs, and indeed the nozzle design itself has an influence [13, 14], but in this work it was decided not to vary either. Clearly for tests on the flat specimens at different angles, part of the specimen then became closer to the nozzle exit and some further away.

2.2 Die Specimens

Two different "die" specimens were used in the testing. In order to achieve contact geometries representative of the wide variety seen in a die both flat and cylindrical shapes were chosen. For the flat specimens different angles could be used. Angle of impact is very important in determining erosive wear behaviour [15, 16]. Previous work has shown, for ductile materials, that wear rates and features change as the counterface specimen is moved from being perpendicular to the erodent flow (where impact craters form with lips which are subsequently removed leading to material removal) to an acute angle to the flow (where wear behaviour becomes almost exclusively about cutting) (see Figure 4 (from [15])). In between a mix of impact and cutting is seen. Hoever, it has been observed that with an erosive wear scar, that wear mechanics particularly where the test surface is not perpendicular, and a variety of modes may be seen. Where the particles initially impact craters are seen, but then lower down the elliptical scars more cutting is seen [17]. Peak wear is seen at around an angle of 30°. It should be noted

that different trends occur for brittle materials where wear mechanisms vary and the peak wear occurs at 90° [16].

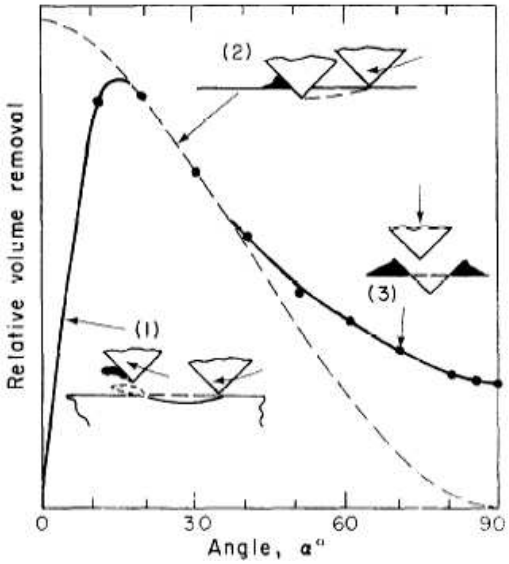

Figure 4. Erosive Impact Wear Behaviour of Ductile Materials with changing Impact Angle [15])

The cylindrical specimens could be set-up to be in alignment or offset from the centre of the nozzle. It was thought possible that the use of the cylindrical specimens could give a variety of contacts and that the full range of erosion mechanisms could be obtained with one specimen. They would also be better for the investigation of temperature effects as a cylindrical resistance heater could be inserted giving a uniform heat distribution that would not be obtained in a flat specimen.

2.3 Aluminium Balls

In order to simulate the metal droplets impacting the die, 6061 aluminium balls (supplied by the Atlas Ball & Bearing Co. Ltd.) were chosen as the test erodent. The balls were 3mm in diameter. This was based on analysis carried out in previous work to determine the size of free droplets of molten aluminium [18].

A question here may arise on how well solid aluminium balls represent the aluminium droplets entering a die during a casting process. Currently there is a trend towards using semi-molten aluminium in casting, which helps with the case for solid balls [19]. Also it has been noted in the literature by several authors that the deformation region at the impact point and consequently the damage caused by liquid and solid droplets is similar [20-22].

Property	Value
Yield Strength (MPa)	103
Ultimate Tensile Strength (MPa)	228
Hardness (Hv)	107
Roughness (Ra, μm)	0.84
Ultimate Shear Strength (MPa)	152

Table 2. Properties of the Aluminium Balls

Initial studies using the rig indicated that with a continuous flow of balls the wear was taking a long time to accumulate. An investigation with a high speed video set-up to determine the impact rate showed that it would need a very large number of balls to keep the impact rate high so it was decided to try a pulsed approach, i.e., fire all the balls in the machine, then stop and allow them to recollect and then re-fire. High speed video indicated that with this method the impact rate was improved, and it is of course far more representative of the situation in an actual casting machine.

Varying ball velocity was thought to be important as within the casting machines this varies with the pressure used in the process of pushing the molten metal into the die. Previous work has shown that wear is approximately $\propto$ velicity^2 [23].

2.4 Ball/Counterface Interaction

The ball/counterface interaction was extensively analysed using a high speed vide technique to assess ball behaviour for all the different set-ups proposed for erosion testing. For the flat specimens this covered the different angles and for the cylindrical specimen this looked at the central and offset positions.

When using the shot-blaster the air pressure could be controlled. High speed video was used to assess what ball impact velocity each setting gave. Richimas v3.2 software was used to determine movement between frames to calculate the velocities. This revealed that the pressures of 20, 40, 60 and 80psi gave ball impact velocities of 9.2, 15.2, 18.4 and 20m/s respectively. The flow rates were also determined for each pressure and there were found to be (in grams of balls per "pulse"): 14, 30, 41 and 55 respectively. This was important to know in analysing the erosive wear rates.

The balls spread a small amount on exiting the nozzle as has been seen in previous work [24, 25]. Although most impacted centrally under the nozzle, the spread meant that across each impact zone the ball behaviour varied. At impact angles of 30° and 60° part of the counterface specimen became closer and part further away than for the 90° case which meant a wider spread in behaviour across the same specimen.

Schematic diagrams illustrating impact behaviour of the balls at impact angles of 30°, 60° and 90° (derived directly from images captured from the high speed video, an example of which is shown in Figure 5) are shown in Figure 6. Generally three different behaviours were seen: impact and a rebound, impact and a slide along the counterface surface and impact and "pressure" applied by subsequent balls. The proportions of each were dictated by the impact angle: more impact and slide on the angled specimens and more "pressure" for the 90° specimen. Where balls accumulated and the "pressure" was apparent, the initial balls provided protection

for the surface from the following balls meaning that there were less direct impacts on the surface. This "umbrella" effect has been described previously [26].

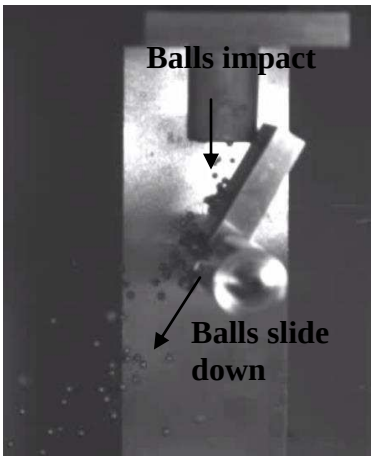

Figure 5. Example Image Captured from the High Speed Image Analysis for a 30° Angle Impact

As shown in Figure 7a, for the specimen located centrally below the nozzle there was a build-up of balls at the initial contact point. From there a few balls rebounded, but most were "pressed" against the specimen with some then sliding down its sides. For the eccentric specimen (see Figure 7b), most rebounded or slid down the side of the specimen. There were no balls "pressured" at the specimen surface.

3 EXPERIMENTAL DETAILS

For the flat specimens, erosion tests were carried out with a nozzle centre distance to the specimen of 30mm at impact velocities of 9.2, 15.2, 18.4 and 20m/s and impact angles of 30°, 60° and 90°. The specimens were made from H13 steel with a hardness of $300H_{V20}$ and an initial roughness (Ra) of 0.6μm.

For the cylindrical specimens, erosion tests were carried out with a central mounting position under the nozzle and with an offset of 5mm from the centre. Velocities of 15.2 and 20m/s were used. The specimens were 10mm in diameter and 70mm long and made from H13 steel with a hardness of $300H_{V20}$. Initial roughness (Ra) in this case was 0.5μm.

For both sets of tests pulsed application of balls was used. The balls were refreshed regularly. Specimens were removed every 1200 pulses for mass measurements (using a balance with an accuracy of 0.00001g). Roughness measurements were taken at the ends of the tests (after 7200 pulses). Surface images were also taken using optical microscopy.

Erosion rates were calculated for each test and were quoted as mass loss per mass of impacting balls:

$$Erosion\ Rate = \frac{mass\ removed}{mass\ of\ balls\ striking\ the\ surface} \quad (1)$$

Repeats were not carried out, although this will be a strong focus in further work. Here the available test resource was focussed on exploring a wide parameter range.

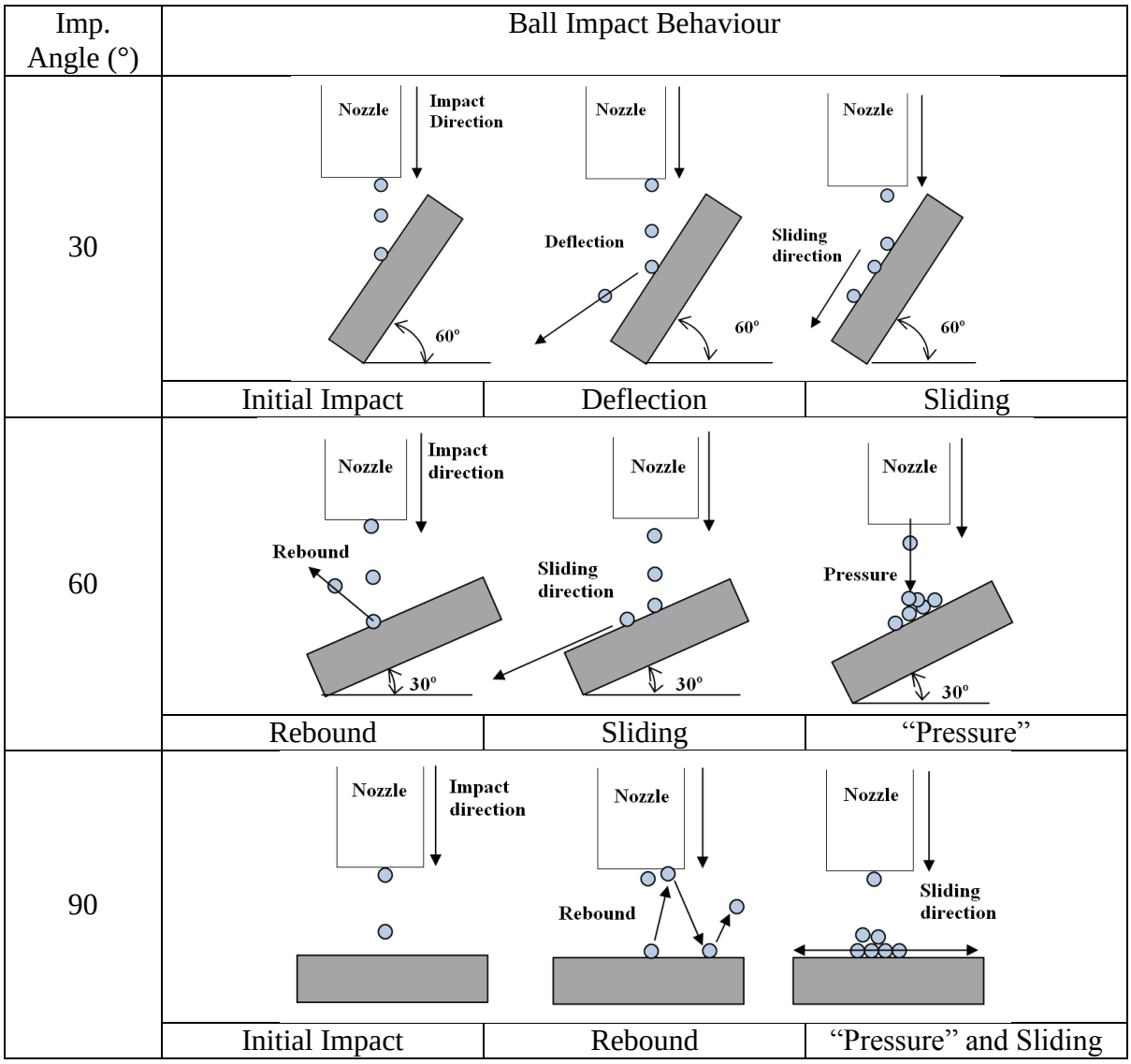

Figure 6. Ball Impact Behaviour against Flat Specimens at a Range of impact Angles

4 RESULTS AND DISCUSSION

4.1 Wear Scar Morphology

The wear scar shapes for the flat specimens from the 90° to 30° degree impact angles changed from circular to elliptical as would have been expected.

In the case of the 30° and 60° impact angles, the wear scars could be split into a top, middle and bottom zone (see Figure 8a) that were characterised by different wear mechanisms as shown in Figures 8b to 8d. These very much aligned with the behaviour seen in the high speed video imaging of the ball impacts outlined in Section 2.4. The middle section is where most balls impacted directly below the nozzle exit. Here the main wear feature was impact craters (see Figure 8c). The top zone had smaller and fewer impact craters as fewer balls were impacting here and had no opportunity to slide as they most likely rebounded (see Figure 8b). The bottom

zone again had less impact craters for the same reason but here there was also evidence of ball sliding as shown in Figure 8d. In Figure 9 a typical cutting gouge formed as a ball impacts and slides is shown with a lip protruding at the bottom. As impact velocity increased the wear scars became larger as the balls spread further, and the wear features seen became larger and deeper and more frequent. The features characterising each zone were the same for each speed. These scars help in working out what mechanisms are prevalent and indicate the effects of different impact angles and speeds, but they do not look similar to those seen in the acual dies (see Figure 2). Very few surfaces that the molten aluminium interacts with are actually flat though, most are curved.

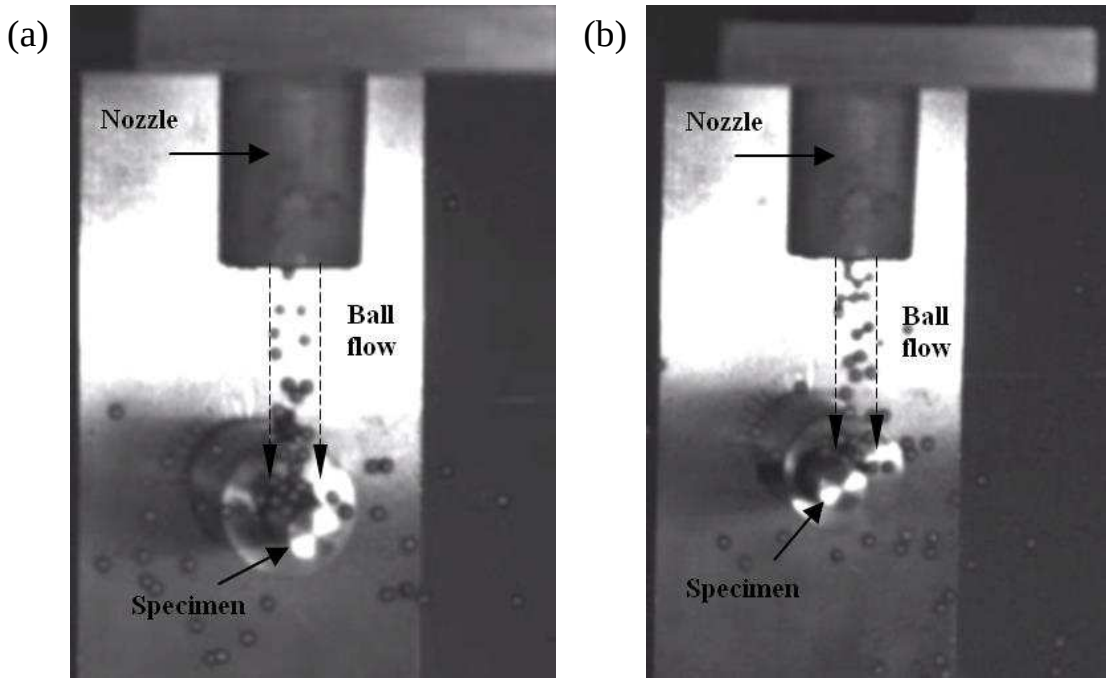

Figure 7. Images Captured from High Speed Video of (a) the Central Specimen and (b) the Eccentric Specimen

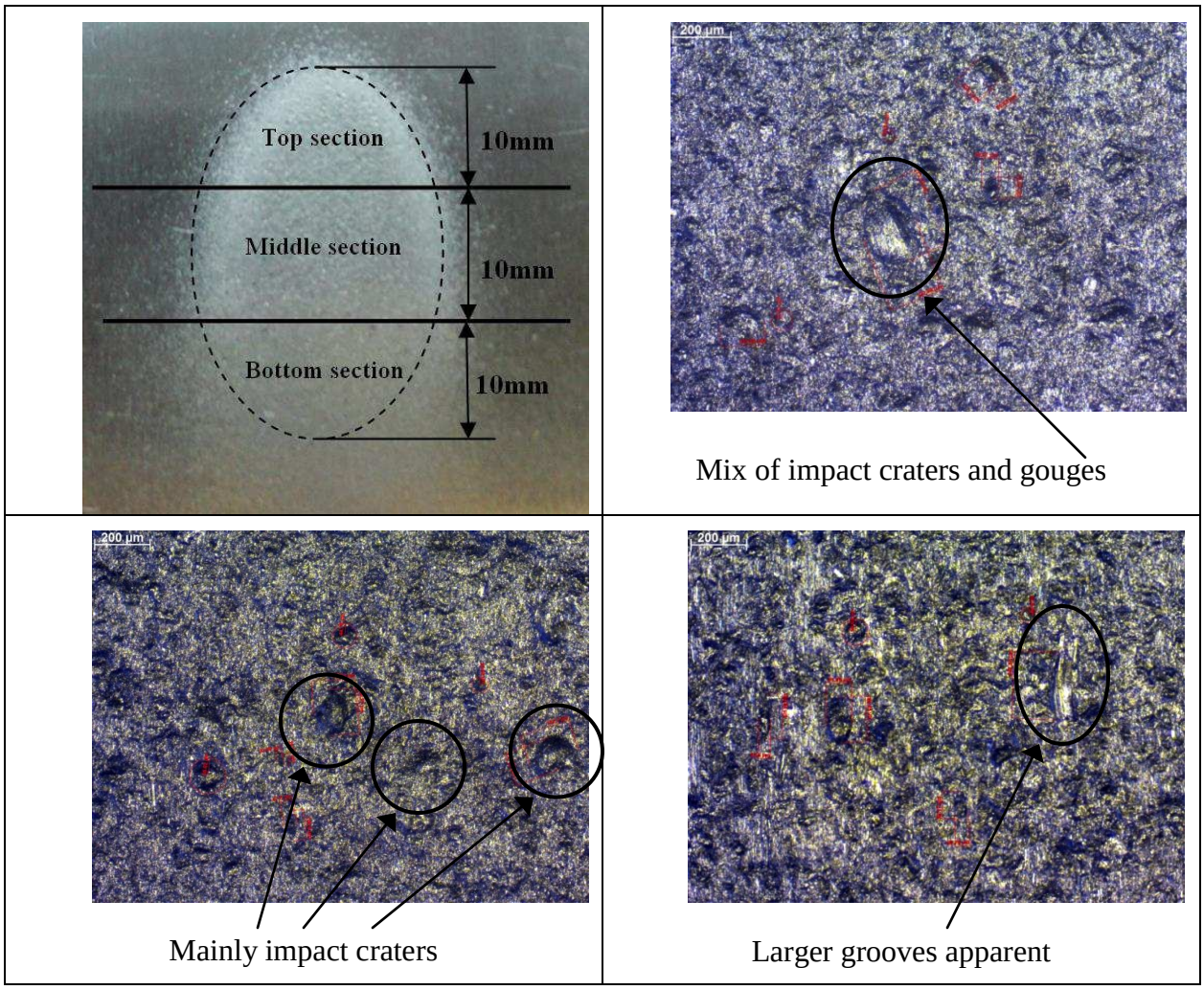

Figure 8. Wear Scar Morphologies: (a) Typical Overall Flat Specimen Scar Split (30°/60° impact angle); 30° Flat Specimen Test at 18.4m/s for the: (b) Top Zone; (c) Middle Zone and (d) Bottom Zone

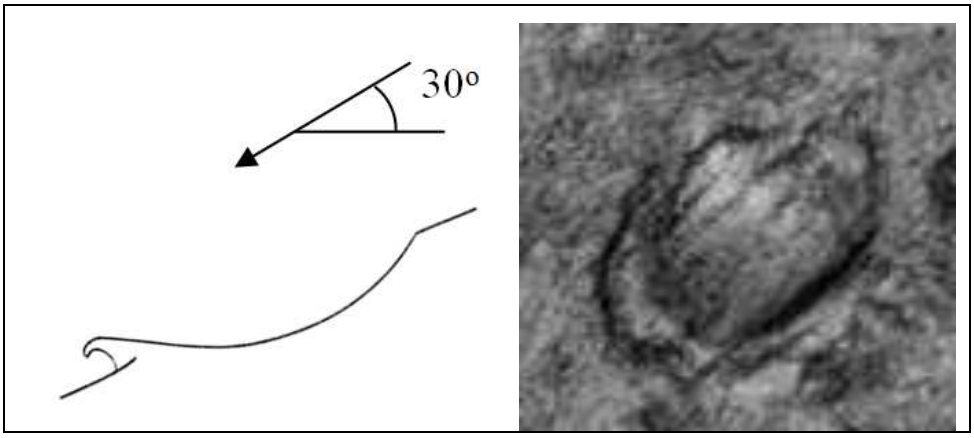

Figure 9. Typical Example of a Cutting Wear Feature from a 60° Impact Test

At an impact angle of 90° the circular wear scars could be split into an outer and inner zone. The inner zone was where most balls impacted. Here there was evidence of many deep craters, lips were also visible in some cases (see Figure 10a). In the outer zone there were fewer impact craters and they were shallower (see Figure 10b).

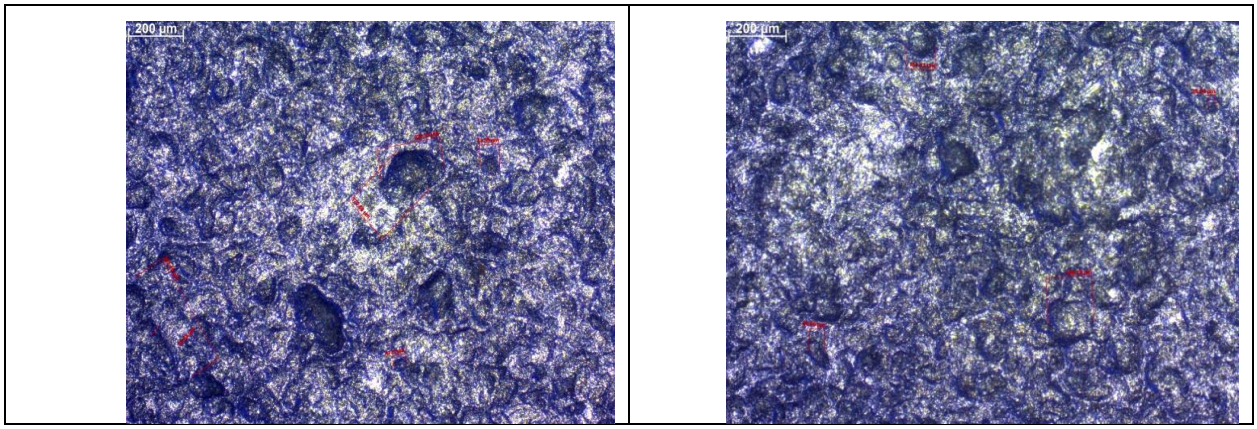

Figure 10. Wear Scar Morphologies for the 90° Flat Specimen Test at 20m/s for the: (a) Inner Zone; (b) Outer Zone

Roughness for the different test set-ups is shown in Figure 11a and the variation across the wear scars for tests at 20m/s in Figure 11b. Clearly impact craters give a higher roughness change than the gouges formed in cutting, as indicated by the higher roughness values for 90° overall and the higher roughness in the tests at 30° and 60° in the central regions where mostly impact only occurred.

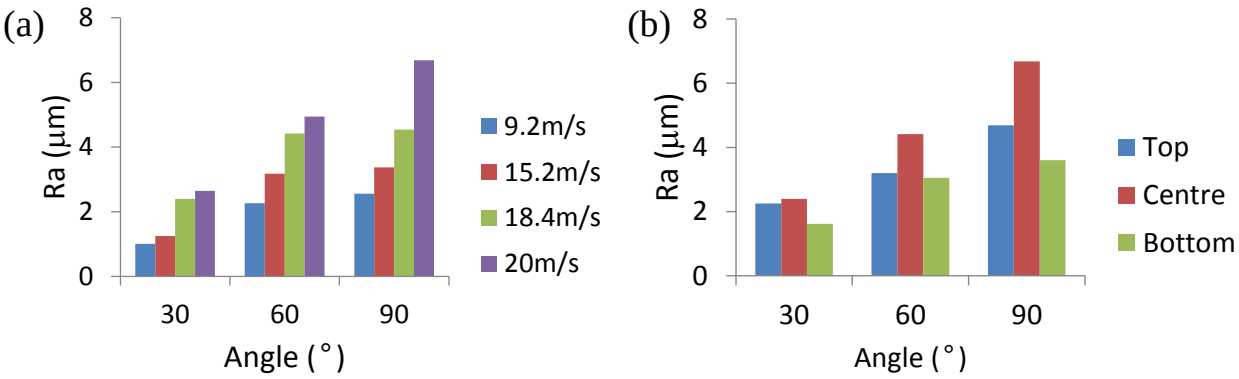

Figure 11. Specimen Roughness (Ra): (a) Average Values for 30°,60°, and 90° Flat Specimens and (b) Comparison of Values for the Top Middle and Bottom Sections of the Flat Specimen Wear Scars from Tests at 20m/s

Figure 12 shows wear scars for cylindrical specimens at a central and eccentric position for an impact velocity of 15.2m/s. The central position scar is larger as more balls are likely to hit it as it is positioned directly under the nozzle. A more detailed outline of the wear scar surfaces is

shown in Figure 13 where top and side views are shown for tests at 15.2m/s. At the top the wear scars are characterised by impact craters and at the sides there are cutting grooves. The grooves were far more predominant for the eccentric test as far more balls are sliding past (see Section 2.4). At the higher speeds, the features, as with the flat specimen case, were larger and deeper. The wear features, particularly the grooves were very similar to those seen in the actual dies (see Figure 2).

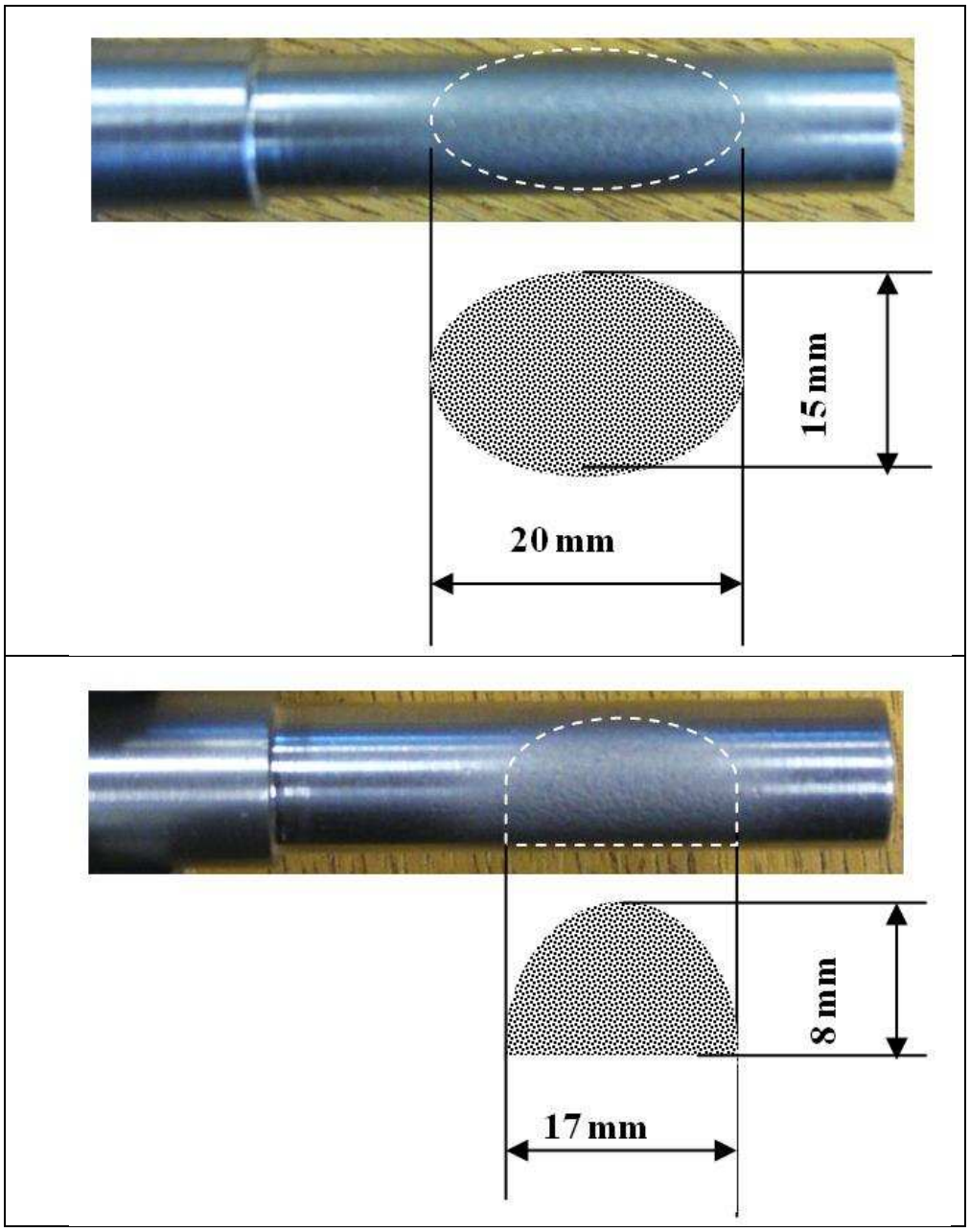

Figure 12. Cylindrical Wear Specimen Wear Scars at 15.2 m/s: (a) Central and (b) Eccentric Positions

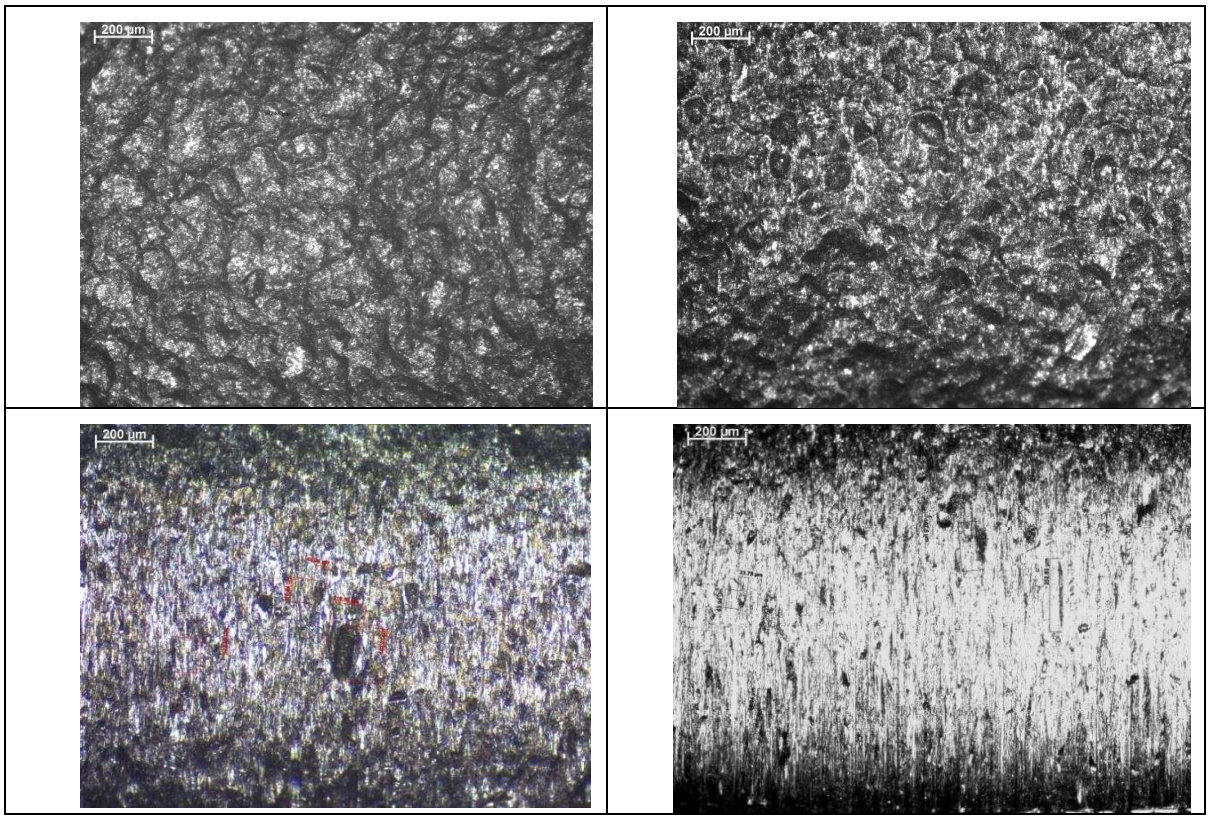

Figure 13. Cylindrical Wear Specimen Wear Scars at 15.2 m/s: (a) Central Top; (b) Central Side; (c) Eccentric Top and (d) Eccentric Side

Variation in roughness around the central and eccentric cylindrical specimens is shown in Figure 14, where the top of the specimen is at 90°. As with the flat specimens the impact craters led to a higher roughness than the cutting at the sides of the specimens. The eccentricity is immediately obvious from the non-symmetrical nature of the data.

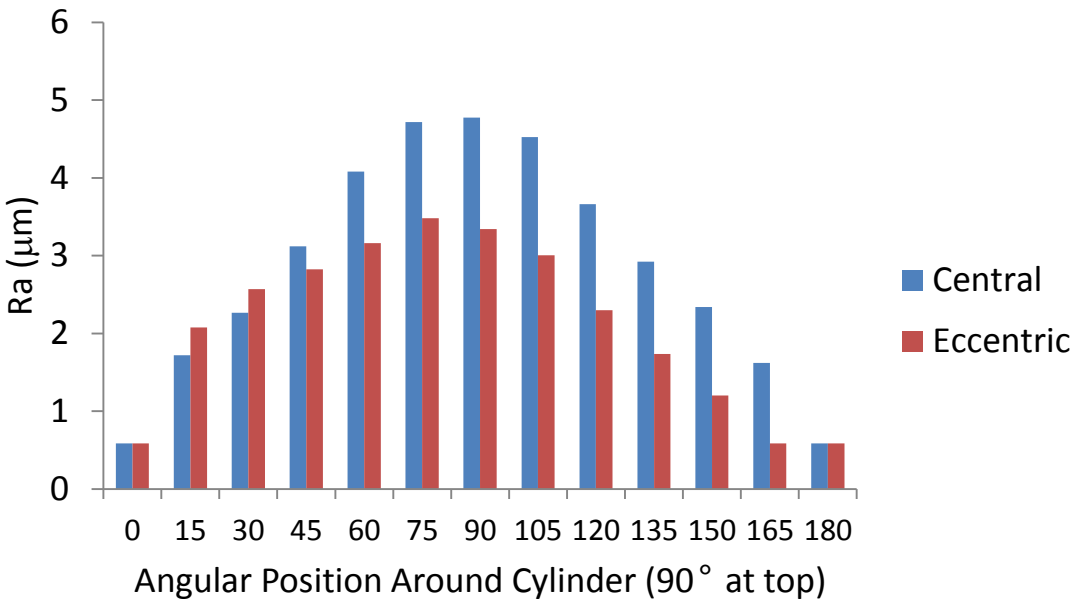

Figure 14. Comparison of Roughness (Ra) Values for Positions around both Cylindrical Central and Eccentric Specimens (90° is the top of the specimen)

4.2 Erosion Rates

Figure 15 shows the erosion rate versus pulse number for the flat specimen tests carried out at 30°; 60° and 90° impact angles. Previous work on the effect of exposure time in liquid and solid particle erosion of ductile materials has highlighted that there are four phases as shown in Figure 16 [27-29]. These are: incubation; acceleration; deceleration and steady state.

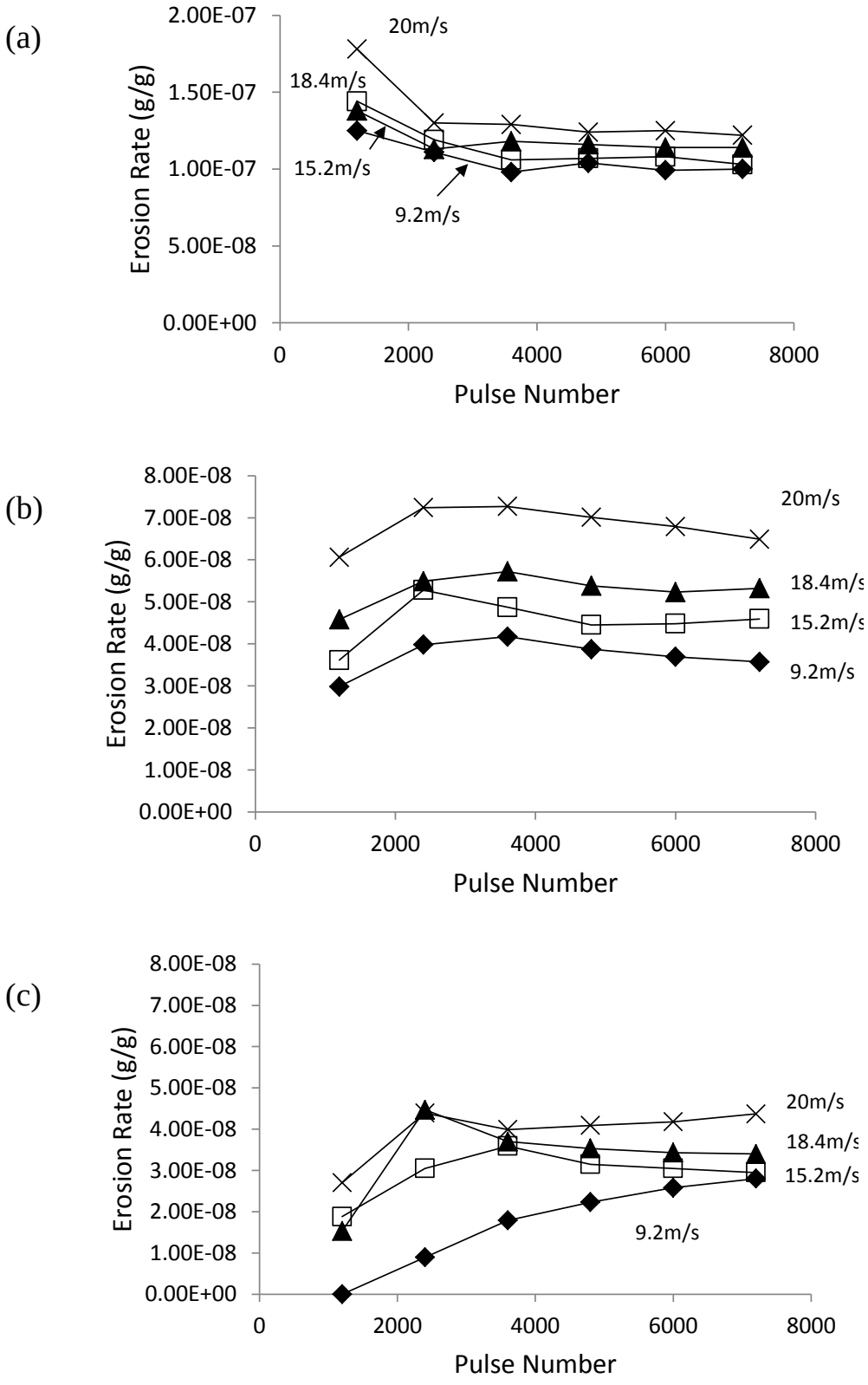

Figure 15. Erosion Rates versus Pulse Number for Flat Specimens at: (a) 30°; (b) 60° and (c) 90° Impact Angles

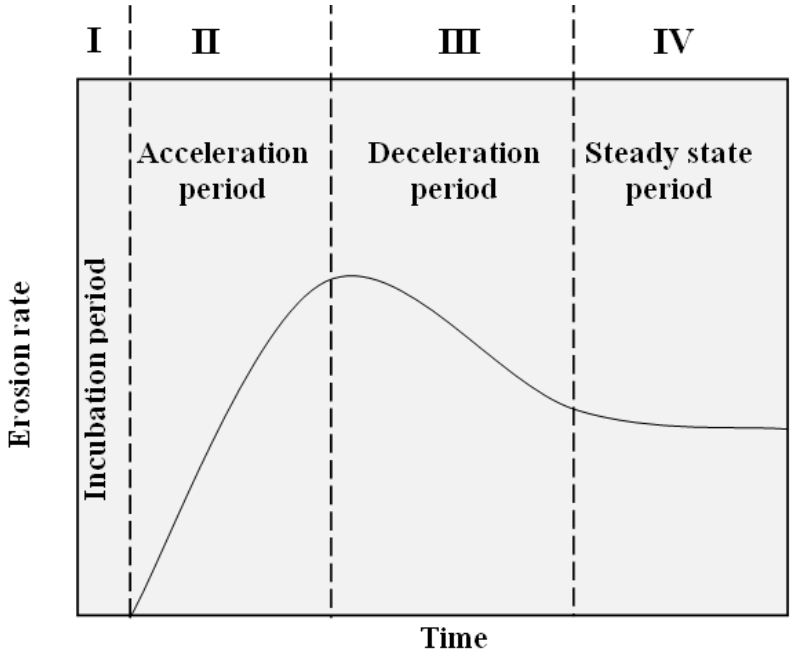

Figure 16. Phases in Erosive Wear (adapted from [27-29])

The data illustrated in Figure 15 shows that for the tests carried out in this study the same phases are apparent. It is clear that for the 30° case that the incubation and acceleration phases have been missed as it must have occurred in the first 1200 cycles before a mass loss measurement was taken. This is not surprising; the wear rate at this angle is much higher than the other two angles, and damage leading to material loss would have occurred much quicker as the balls are sliding and cutting the specimen rather than impacting and forming craters (see surface images in Figure 8). At 60° the incubation period was longer, but still shorter than that at 90°. Some cutting occurs, but in combination with a greater amount of impact crater formation. Crater formation does not lead to material loss quickly as balls have to impact the lips formed and break them away before they contribute to the overall mass loss. The incubation period, does, however, as shown in Figure 15, shorten with higher impact velocities. At 90° and low speed the incubation period is not over by the end of the tests. At higher speed the greater impact energy leads to larger craters with bigger lips that break away more quickly leading to the acceleration phase occurring more quickly.

As shown in Figure 17, the erosion versus impact angle behaviour follows the trends observed in previous work [15, 16] in that the peak wear occurs at 30°. Figure 18 shows how erosion rate progresses with increasing impact velocity for the three impact angles tested. The rate of increase does not match those observed in previous tests.

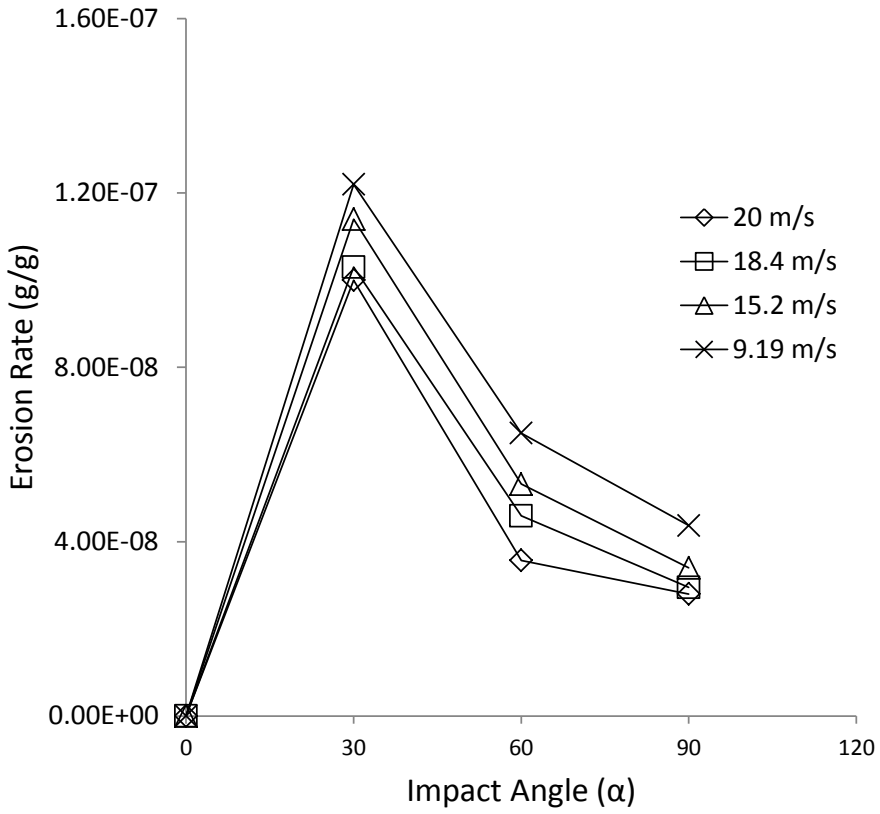

Figure 17. Flat Specimen Impact Angle against Erosion Rate for Impact Velocities of 9.2, 15.2, 18.4 and 20m/s

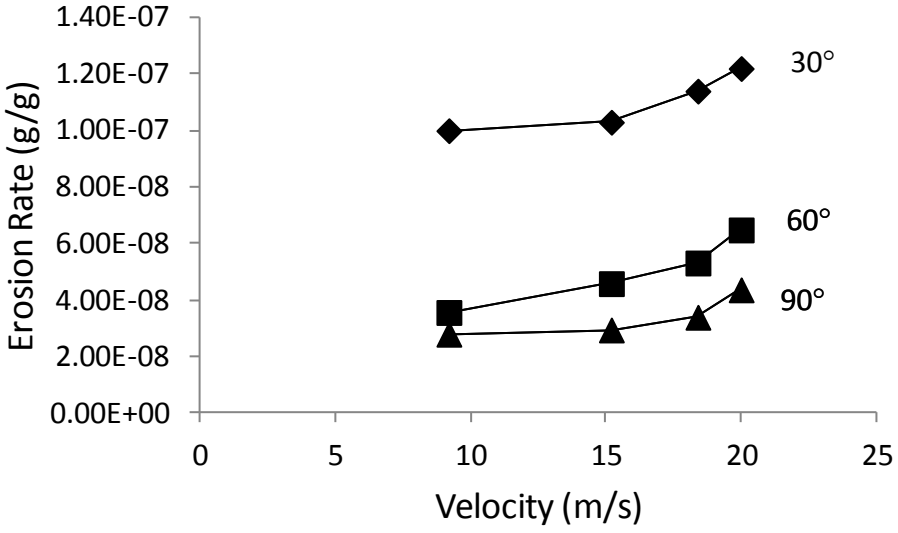

Figure 18. Erosion Rate against Impact Velocity for Flat Specimen Impact Angles of 30°,60°, and 90°

Figure 19 shows the erosion rates for the centrally located and eccentric specimens. The central specimen wore less and showed evidence of following the phases outlined above that were seen for the flat specimens.

Erosion rates for the eccentric specimen indicated that if an incubation period occurred it happened before 1200 cycles. Wear, as shown, continued to rise after initiating. This is not unexpected because as most balls are make acute angle contacts and sliding past (as with the 30° flat specimen where a similar short acceleration of wear was seen) (as noted in Section 2.4) they will cut from the start of the test and continue to cut as the test progresses. In the case of the central specimen, wear rates would take longer to rise because of the impact component and the time taken for crater lips to detach. Erosion rate is more likely to plateau due to work hardening caused by the impacts. The changing geometry due to wear would also contribute. For the eccentric specimen the greater side wear would lead to greater sliding contact. The wear at the top of the central specimen would probably reduce the likelihood of sliding happening (see diagrams on Figure 19).

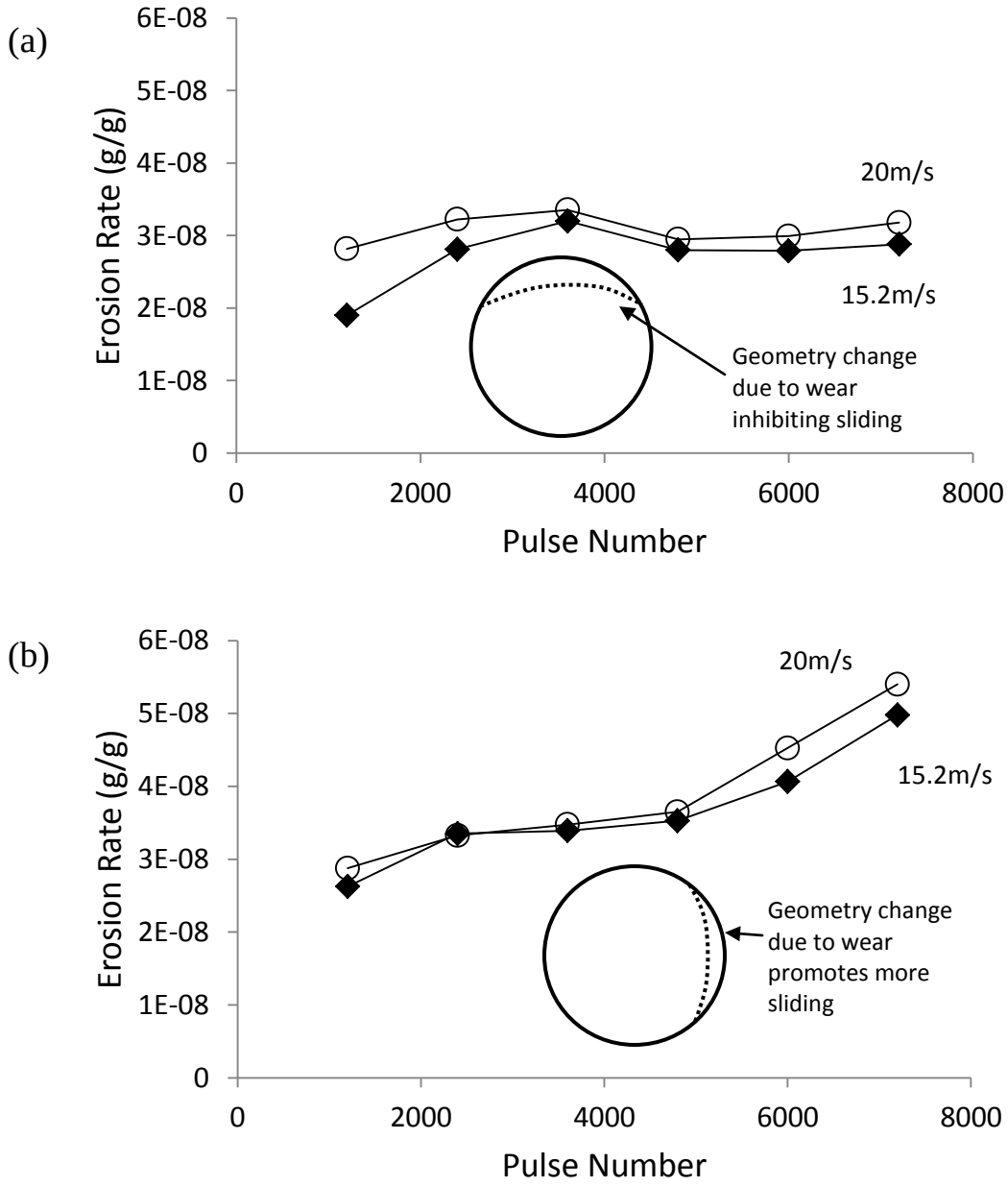

Figure 19. Cylindrical Specimen Erosion Rate versus Pulse Number for (a) Central and (b) Eccentric Positions

5 CONCLUSIONS

The aim of the work outlined in this paper was to develop a methodology for assessing erosive wear of dies used in high pressure, cold chamber aluminium casting. Previous tests have either been too simplistic or overly complex and costly as well as time consuming. Here the target was to have a laboratory method that contained more elements of the contact conditions that exist in the actual machine while still being practical and easy to implement.

This was achieved using a commercial shot blaster to apply solid 3mm diameter aluminium balls (thought appropriate to simulate the molten/semi-solid aluminium droplets that impact the dies in the casting machine) in pulses to represent the cyclic impacts seen in the machine. Two types of H13 die steel specimen were tested – flat (at different impact angles) and cylindrical in a central and eccentric position.

In both methods surface features characteristic of those seen in actual dies were achieved. However, the cylindrical specimens were more representative, as in most dies flat surfaces are not found at the critical wear locations.

Trends similar to those seen in other erosion work involving ductile materials were observed. The same incubation, acceleration, deceleration and steady state wear phases occurred, except for the eccentric cylindrical specimen where most balls were impacting, sliding and cutting immediately meaning that material removal was happening throughout the test. In the other tests, where impact was more dominant, material loss did not occur until lips from the craters were removed. Work hardening probably led to the eventual steady state wear rates seen.

For the flat specimens peak wear rates occurred at an impact angle of 30° in line with previous work. Erosion rate rose when impact velocity was increased, but not at the same rate seen in before.

Overall the test method is concluded to be a good representation of the erosion seen in aluminium casting dies and the method can now be taken forward to assess potential solutions to the die erosion problem. The most appropriate specimen was the eccentric cylindrical specimen.

REFERENCES

[1] E.J. Vinarcik, High integrity die casting processes, John Wiley Press, New York, 2002.

[2] A. Street, The Die Casting Book, Portcullis Press Ltd., Redhill, England, 1977.

[3] H. Doehler, Die Casting, McGraw Hill Book Company, New York, 1951.

[4] D.F. Allsop, D. Kennedy, Pressure Die Casting, Part 2: The Technology of the Casting and the Die, Pergamon Press, Oxford, 1983.

[5] M. Yu, M., Shivpuri, R., Rapp, R., Effects of molten aluminium on H13 dies and coatings, Journal of Materials Engineering and Performance 4 (1995) 175-181.

[6] D. Heim, F. Holler, C. Mitterer, Hard coatings produced by PACVD applied to aluminium die casting, Surface and Coatings Technology 116-119 (1999) 530-536.

[7] O. Salas, K. Kearns, S. Carrera, J. J. Moore, tribological behavior of candidate coatings for aluminium die casting dies, Surface and Coatings Technology 172 (2003) 117-127.

[8] K.S. Klimeket, A. Gebauer, P. Kaestner, K.T. Rie, Duplex-PACVD coating of surfaces for die casting tools, Surface and Coatings Technology 201 (2007) 5628-5632.

[9] A. Lousa, J. Romero, E. Martínez, J. Esteve, F. Montalà, L. Carreras, Multilayered chromium/chromium nitride coatings for use in pressure die-casting, Surface and Coatings Technology 146–147 (2001) 268-273.

[10] K.T. Rie, C. Pfohl, S. H. Lee, C. S. Kang, Development of zirconium and boron containing coatings for the application on aluminium die casting tools by means of MO–PACVD, Surface and Coatings Technology 97 (1997) 232-237.

[11] J.R. Laguna-Camacho, L.A. Cruz-Mendoza, J.C. Anzelmetti-Zaragoza, A. Marquina-Chávez, M. Vite-Torres, J. Martínez-Trinidad, Solid particle erosion on coatings employed to protect die casting molds, Progress in Organic Coatings 74 (2012) 750-757.

[12] R. Shivpuri, Y.L. Chu, K. Venkatesan, J.R. Conrad, K. Sridharan, M. Shamim, R.P. Fetherston, An evaluation of metallic coatings for erosive wear resistance in die casting applications, Wear 192 (1996) 49-55.

[13] L. Lapides, A. Levy, The halo effect in jet impingement solid particle erosion testing of ductile metals, Wear 58 (1980) 301-311.

[14] P.H. Shipway, I.M. Hutchings, Influence of nozzle roughness on conditions in a gas-blast erosion rig, Wear 162-164 (1993) 148-158.

[15] I. Finnie, Some reflections on the past and future of erosion, Wear. 186-187 (1995) 1-10.

[16] G.L. Sheldon, I. Finnie, On the ductile behaviour of nominally brittle materials during erosive cutting, Trans. ASME 888 (1966) 387-392.

[17] J. Camacho, R. Lewis, R.S. Dwyer-Joyce, Solid particle erosion caused by rice grains, Wear 267 (2009) 223-232.

[18] R. Ghafouri-Azar, S. Shakeri, S. Chandra, J. Mostaghimi, Interactions between molten metal droplets impinging on a solid surface, International journal of Heat and Mass transfer 46 (2003) 1395-1407.

[19] M. Ramadan, M. Takita, H. Nomura, Effect of semi-solid processing on solidification microstructure and mechanical properties of gray cast iron, Materials Science and Engineering A 417 (2006) 166–173.

[20] H.W. Bargmann, On the time-dependence of the erosion rate – a probabilistic approach to erosion, Theoretical and Applied Fracture Mechanics 6 (1986) 207-215.

[21] H.W. Bargmann, The mechanics of erosion by liquid and solid impact, International Journal of Solids and Structures 29 (1992) 1685-1698.

[22] D.R. Andrews, J.E. Field, The erosion of metals by the normal impingement of hard solid spheres, Journal of Physics 5 (1982) 571-578.

[23] ASM, ASM Handbook Vol. 18 Friction, Lubrication and Wear Technology, ASM International, United States, 1992.

[24] G.P. Tilly, W. Sage, The interaction of particle and material behaviour in erosion processes, Wear 16 (1970) 447-465.

[25] L. Lapides, A. Levy, The halo effect in jet impingement solid particle erosion testing of ductile metals, Wear 58 (1980) 301-311.

[26] K. Anand, S.K. Hovis, H. Conrad, R.O. Scattergood, Flux effects in solid particle erosion, Wear 118 (1987) 243-257.

[27] P.V. Rao, D.H. Buckley, Time dependence of solid-particle impingement erosion of an aluminium alloy, National Aeronautics and Space Administration, Scientific and Technical Information Branch, 1983.

[28] F.J. Heymann, Toward quantitative prediction of liquid impact erosion, ASTM STP474, 1970.

[29] A. Perssona, J. Bergstrom, C. Burmana, S. Hogmark, Influence of deposition temperature and time during PVD coating of CrN on corrosive wear in liquid aluminium, Surface and Coatings Technology. 146 –147 (2001) 42–47.